

Capillary Electrophoresis Frontal Analysis for Characterization of $\alpha_v\beta_3$ Integrin Binding Interactions

Ying Sun,[†] Sonya Cressman,[‡] Ning Fang,[†] Pieter R. Cullis,^{‡,§} and David D. Y. Chen^{*†}

Department of Chemistry, Department of Biochemistry, and Centre for Drug Research and Development, University of British Columbia Vancouver, BC, Canada V6T 1Z3

The specific binding characteristics of $\alpha_v\beta_3$ integrins with an arginine-glycine-aspartic-acid (RGD) containing fluorescently labeled cyclic peptide is investigated with capillary electrophoresis-frontal analysis method. The new algorithm used to calculate the binding constants and binding stoichiometry was derived without the assumptions made in the commonly used Scatchard Plot method, thus enabling the determination of specific binding parameters in the presence of nonspecific binding. The $\alpha_v\beta_3$ integrin, a membrane protein, was studied in solution, without the need of immobilization or any other kind of modification. An RGD containing fluorescently labeled cyclic pentapeptide is used as the ligand with both specific and nonspecific binding characteristics, and an arginine-alanine-aspartic-acid (RAD) containing peptide is used as the control for nonspecific binding. While a typical specific binding isotherm has a shape of a rectangular hyperbola, a nonspecific binding isotherm is linear in the same ligand concentration region. A 1:2 specific binding stoichiometry was revealed with the second binding having a similar affinity compared to the first binding event.

Binding affinity and interaction stoichiometry are essential characteristics for biochemical processes. A variety of methods have been developed to characterize biomolecular interactions, such as equilibrium dialysis, ultrafiltration, ultracentrifugation, gel filtration, calorimetry, microdialysis, spectroscopy, high performance liquid chromatography (HPLC), surface plasmon resonance (SPR), and capillary electrophoresis (CE).^{1–5} CE has many advantages over other techniques, because of the relatively short analysis time, low sample consumption, ease of automation, and high separation efficiency.

Integrins are a large family of heterodimeric integral membrane proteins that function to sense and respond to the extracellular environment.⁶ High levels of $\alpha_v\beta_3$ integrin are expressed in vascular endothelial cells involved in pathological angiogenesis that supports tumor growth, making this class of integrin an attractive anticancer target.^{7,8}

Studies have shown that arginine-glycine-aspartic-acid (RGD) containing peptides can compete with the natural ligands of $\alpha_v\beta_3$ integrins. Potent and specific $\alpha_v\beta_3$ antagonists have been discovered from NMR structural studies.⁹ This has led to the development of Merck's drug candidate, Cilengitide (cyclic arginine-glycine-aspartic-acid-D-phenylalanine-(N-methyl)-lysine (cRGDf-[N(Me)]V)). Second generation conjugates that are similar to Cilengitide have broadened the application of these ligands from just being integrin antagonists to drug delivery and tumor imaging agents.^{10,11}

Despite extensive efforts toward finding integrin antagonists and the existence of high-resolution structural data of the integrin, our understanding of the mechanisms that govern the integrin's switch from an inactive to high-affinity active state is far from complete.¹² In an effort to obtain further insight into the binding of RGD peptides to the integrin, we used solubilized $\alpha_v\beta_3$ integrin and measured RGD binding using CE-FA.

Currently, several CE methods are available to study the equilibrium and kinetic binding properties^{13–18} such as normal affinity CE (ACE), the Hummel–Dreyer method (HD), vacancy

* To whom correspondence should be addressed. Telephone: +01 (604) 822-0878. Fax: +01 (604) 822-2847. E-mail: chen@chem.ubc.ca.

[†] Department of Chemistry.

[‡] Department of Biochemistry.

[§] Centre for Drug Research and Development.

- (1) Bertucci, C.; Domenici, E. *Curr. Med. Chem.* **2002**, *9*, 1463–1481.
- (2) Seville, B.; Zini, R.; Madjar, C. V.; Thuaud, N.; Tillement, J. P. *J. Chromatogr., Biomed. Appl.* **1990**, *531*, 51–77.
- (3) Harding, S. E.; Chowdhry, B. Z. *Protein-Ligand Interactions: Hydrodynamics and Colorimetry*; Oxford University Press: Oxford, 2001.
- (4) Connors, K. A. *Binding Constant. The Measurement of Molecular Complex Stability*; John Wiley & Sons: New York, 1987.
- (5) Oravcova, J.; Bohs, B.; Lindner, W. *J. Chromatogr., Biomed. Appl.* **1996**, *677*, 1–28.

- (6) Giancotti, F. G.; Ruoslahti, E. *Science* **1999**, *285*, 1028–1032.
- (7) Brooks, P. C.; Clark, R. A. F.; Cheresch, D. A. *Science* **1994**, *264*, 569–571.
- (8) Folkman, J. *J. Natl. Cancer Inst.* **1990**, *82*, 4–6.
- (9) Dechantreiter, M. A.; Planker, E.; Matha, B.; Lohof, E.; Holzemann, G.; Jonczyk, A.; Goodman, S. L.; Kessler, H. *J. Med. Chem.* **1999**, *42*, 3033–3040.
- (10) Beer, A. J.; Haubner, R.; Sarbia, M.; Goebel, M.; Luderschmidt, S.; Grosu, A. L.; Schnell, O.; Niemeyer, M.; Kessler, H.; Wester, H. J.; Weber, W. A.; Schwaiger, M. *Clin. Cancer Res.* **2006**, *12*, 3942–3949.
- (11) Wu, Y.; Cai, W.; Chen, X. *Mol. Imaging Biol.* **2006**.
- (12) Puklin-Faucher, E.; Gao, M.; Schulten, K.; Vogel, V. *J. Cell Biol.* **2006**, *175*, 349–360.
- (13) Rundlett, K. L.; Armstrong, D. W. *Electrophoresis* **1997**, *18*, 2194–2202.
- (14) Rundlett, K. L.; Armstrong, D. W. *Electrophoresis* **2001**, *22*, 1419–1427.
- (15) Petrov, A.; Okhonin, V.; Berezovski, M.; Krylov, S. N. *J. Am. Chem. Soc.* **2005**, *127*, 17104–17110.
- (16) Galbusera, C.; Chen, D. D. Y. *Curr. Opin. Biotechnol.* **2003**, *14*, 126–130.
- (17) Heegaard, N. H. H.; Nissen, M. H.; Chen, D. D. Y. *Electrophoresis* **2002**, *23*, 815–822.
- (18) Busch, M. H. A.; Kraak, J. C.; Poppe, H. *J. Chromatogr. A* **1997**, *777*, 329–353.

affinity CE (VACE), the vacancy peak method (VP), and frontal analysis (CE-FA).^{19–21} The most suitable method can be chosen based on the characteristics of the binding interaction, namely, the speed of the association/dissociation processes, the mobilities of the free species and the complex, each species' ability to absorb UV light or emit fluorescence, and the availability of the interacting species. In ACE and VACE methods, measurable differences in electrophoretic mobilities between free ligand and the complex are required, and the measurements are based on the changes in electrophoretic mobility of free protein or ligand due to complex formation.^{18,21–23} In HD and VP methods, the mobilities of free protein and the complex have to be similar, and the measurements are mainly based on the changes of the free ligand concentration.

In CE-FA, a relatively large amount (~100 nL) of a pre-equilibrated mixture of protein and ligand is injected into the capillary filled with background electrolyte (BGE). The injection of a large volume of a sample plug leads to the appearance of plateaus in the observed electropherogram. Partial separation of the binding species can be achieved based on the differences in their mobilities. The compound with a unique mobility in the capillary is separated from the mixture plateau to form another plateau. In the study of protein and ligand interaction, the mobility of the free ligand is usually different from those of the protein and the protein–ligand complex. The height of the plateau is directly related to the concentration of corresponding species; therefore, the binding parameters can be determined by comparing the heights of the plateaus.

Different data analysis methods have been utilized to estimate binding parameters in CE.²² With the papers published to date, a complex equilibrium model based on Scatchard analysis has been the most commonly used in CE-FA.²⁴ According to the assumptions used in this approach, binding parameters can be obtained in cases where the binding stoichiometry is 1:1 and where noncooperative binding occurs on multiple identical binding sites. However, there are many other cases relevant to biomolecules that do not fit the interaction model described.²⁵ Specific binding and nonspecific binding often coexist in protein–ligand interactions, and methods need to be developed to differentiate the different types of binding because, in many occasions, only specific bindings trigger the cascade of biochemical processes.

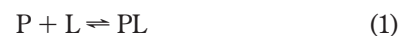
In this study, we have found new information about the binding of cRGDFK-448 to the $\alpha_v\beta_3$ integrin as measured by the CE-FA method. This behavior was characterized by a set of refined equations for determining the parameters of higher order binding.

THEORY

Currently, the most often used approach to determining the binding characteristics for interactions with higher order stoichiometry is to evaluate the changes of a physical parameter of the system with a Scatchard Plot.⁴ For a Scatchard Plot to provide

meaningful information, certain conditions have to be satisfied. The ligand should have only one active site, and the multiple binding sites on the protein should be identical, distinguishable, and independent. However, in practice, these conditions may not be easily met. Specific binding events often differ from nonspecific ones, and the binding of the first ligand often affects the second binding, favorably or adversely, depending on the property of the protein. To properly account for these interactions, the following equations are derived and used to process the data obtained in this work.

As the binding of the species (protein–ligand) occurs with a 1:1 stoichiometry, the equilibrium is given by



$$K_b = \frac{[PL]}{[P][L]} \quad (2)$$

where [P], [L], and [PL] are the concentrations of the protein, the ligand, and the protein–ligand complex, respectively. The binding constant, K_b , is given by eq 2. The fraction of the protein bound, $f_{b,P}$, is an important factor that can be used to determine the affinity between the protein and the ligand:

$$f_{b,P} = \frac{[P]_b}{[P]_t} = \frac{[PL]}{[P]_f + [PL]} \quad (3)$$

The subscripts b, f, and t denote bound, free, and total concentrations of corresponding species in the solution, respectively. In CE-FA, the injected sample plug contains pre-equilibrated protein and ligand. The total concentration of protein present in the sample mixture, $[P]_t$, is kept constant, and the total ligand concentration, $[L]_t$, is varied in each CE process. As the species start to migrate through the capillary under a high voltage, the free ligand molecules are partially separated from the protein and the protein–ligand complex. As shown in Figure 1A, the free ligand concentration can be calculated by using a common calibration curve, obtained by injecting samples containing only the ligand. The calculated $[L]_f$ can be used to estimate the binding parameters. In CE-FA, $[P]_b$ is always difficult to determine because the mobilities of free protein and protein–ligand complex are often very close, and the two species are present in the same mixture. Therefore, the average number of ligand molecules bound per protein molecule, I , is introduced as $[L]_b/[P]_t$ based on the relation of $[P]_b$ and $[L]_b$ in different interaction stoichiometries. For a 1:1 binding, $[L]_b$ is equal to $[P]_b$, which is also the concentration of the complex formed, [PL]; I can be written as

$$I = \frac{[L]_b}{[P]_t} = \frac{[PL]}{[P]_f + [PL]} = \frac{K_b[L]_f}{1 + K_b[L]_f} \quad (4)$$

With a plot of $[L]_b/[P]_t$ vs $[L]_f$, the binding constant, K_b , can be determined by a nonlinear curve fit.

Higher Order Binding Stoichiometry. Specific binding of small molecules to macromolecules, such as enzymes and other proteins, polynucleic acids, and synthetic polymers, is an important area that often requires consideration of multiple binding sites.²⁶

- (19) Kraak, J. C.; Busch, S.; Poppe, H. J. *Chromatogr.* **1992**, *608*, 257–264.
 (20) Busch, M. H. A.; Boelens, H. F. M.; Kraak, J. C.; Poppe, H. J. *Chromatogr. A* **1997**, *775*, 313–326.
 (21) Busch, M. H. A.; Carels, L. B.; Boelens, H. F. M.; Kraak, J. C.; Poppe, H. J. *Chromatogr. A* **1997**, *777*, 311–328.
 (22) Tanaka, Y.; Terabe, S. J. *Chromatogr., B: Anal. Technol. Biomed. Life Sci.* **2002**, *768*, 81–92.
 (23) Rundlett, K. L.; Armstrong, D. W. *Electrophoresis* **2001**, *22*, 1419–1427.
 (24) Ostergaard, J.; Heegaard, N. H. H. *Electrophoresis* **2003**, *24*, 2903–2913.
 (25) Bowser, M. T.; Chen, D. D. Y. *Anal. Chem.* **1998**, *70*, 3261–3270.

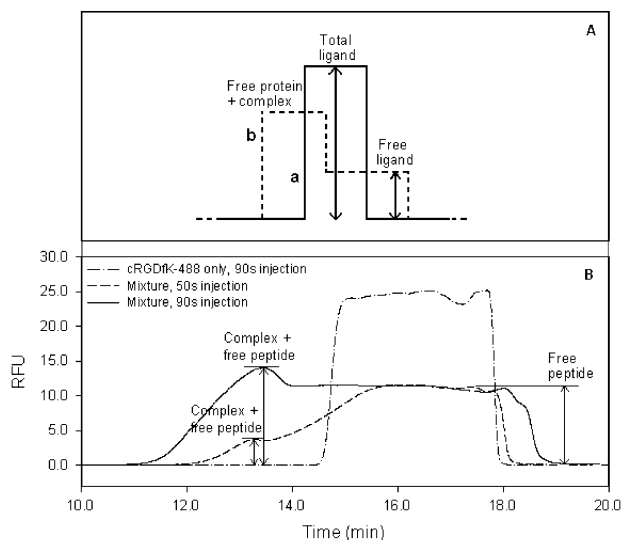


Figure 1. Ideal and experimental CE-FA profiles. (A) Ideal signal profile from a set of CE frontal analysis experiments. The heights of the rectangular signals are directly related to the concentration of corresponding species. The solid curve (a) is for sample containing ligand only, and the dashed curve (b) represents the sample containing a pre-equilibrated mixture of protein and ligand. When a portion of the ligand formed the complex in the pre-equilibrated sample plug, the height of plateau resulted from the unbound peptide, $[L]_f$, decreased. The increased migration time of the free peptide is caused by the reduced electroosmotic flow when a large plug of protein and ligand mixture is present during the CE process. (B) The plateau height (dash-dot curve) results from a free cRGDFK-488 peptide plug at $2.40 \mu\text{M}$ with a 90 s injection under a pressure of 0.5 psi. The other two curves resulted from the injection of the pre-equilibrated mixture of integrin ($0.295 \mu\text{M}$) and peptide ($2.40 \mu\text{M}$) but with different injection times: 90 s (solid) and 50 s (dash).

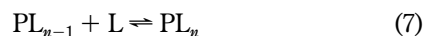
A Scatchard plot ($[L]_b/[L]_f$ vs $[L]_b$) has been used to process data obtained by CE methods such as CE-FA, HD, and VP.^{23,27,28}

Because the assumptions used in the Scatchard method are often not valid for biological molecules, a more general model should be developed. For a 1:2 interaction, eqs 1 and 2 can be used to describe the first binding step, with K_{b1} replacing K_b as the binding constant. The following binding events can be described as the following:



$$K_{b2} = \frac{[\text{PL}_2]}{[\text{PL}][\text{L}]_f} \quad (6)$$

and



$$K_{bn} = \frac{[\text{PL}_n]}{[\text{PL}_{n-1}][\text{L}]_f} \quad (8)$$

The overall binding constant, K , is generally calculated as the product of binding constants of each step:

$$K = \prod_{n=1}^N K_{bn} = K_{b1} \cdot K_{b2} \cdot K_{bn} = \frac{[\text{PL}_n]}{[\text{P}]_f [\text{L}]_f^n} \quad (9)$$

In this study, we will focus on the specific interaction with a small number of binding sites (i.e., $n = 2$ and/or 3), which is common for binding of macromolecules in real biological systems. For a protein–ligand binding with a 1:2 or 1:3 stoichiometry, inserting $[\text{PL}]$, $[\text{PL}_2]$, and $[\text{PL}_3]$ into eq 9, the I value for a 1:2 binding is obtained from

$$I = \frac{[\text{L}]_b}{[\text{P}]_t} = \frac{[\text{PL}] + 2[\text{PL}_2]}{[\text{P}]_f + [\text{PL}] + [\text{PL}_2]} = \frac{K_{b1}[\text{L}]_f + 2K_{b1}K_{b2}[\text{L}]_f^2}{1 + K_{b1}[\text{L}]_f + K_{b1}K_{b2}[\text{L}]_f^2} \quad (10)$$

and the I value for a 1:3 binding is obtained from

$$I = \frac{[\text{L}]_b}{[\text{P}]_t} = \frac{[\text{PL}] + 2[\text{PL}_2] + 3[\text{PL}_3]}{[\text{P}]_f + [\text{PL}] + [\text{PL}_2] + [\text{PL}_3]} = \frac{K_{b1}[\text{L}]_f + 2K_{b1}K_{b2}[\text{L}]_f^2 + 3K_{b1}K_{b2}K_{b3}[\text{L}]_f^3}{1 + K_{b1}[\text{L}]_f + K_{b1}K_{b2}[\text{L}]_f^2 + K_{b1}K_{b2}K_{b3}[\text{L}]_f^3} \quad (11)$$

For the case of multiple types of binding sites, the overall I can be defined as

$$I_t = \sum_{i=1}^m I_i \quad (12)$$

Most commonly, i is 1 or 2 as reported in the literature. If nonspecific binding also exists, I is the sum of I_{specific} and $I_{\text{nonspecific}}$, and eqs 4, 10, and 11 still describe the specific binding process, if the nonspecific binding can be accounted for. Thus, the appropriate isotherm describing a higher order equilibrium for each type of sites is generalized:

$$I = \frac{\sum_{n=1}^N nK_n[\text{L}]_f^n}{1 + \sum_{n=1}^N K_n[\text{L}]_f^n} \quad (13)$$

Most of the parameters in eq 13 are defined earlier, except for N , which is the maximum number of binding sites available on each protein molecule. The individual binding constant for each step, K_{bn} , can be determined by plotting $[\text{L}]_b/[\text{P}]_t$ vs the free ligand concentration, $[\text{L}]_f$, and the number of binding sites can be determined by fitting the experimental results with the n th order equation, such as eqs 10, 11, and 13. It should be noted that the unit of the binding constant obtained from Scatchard plots is always in M^{-1} , forcing all multiple bindings to a pseudo 1:1 stoichiometry. The overall binding constant obtained by eqs 4, 10, and 11 have units of M^{-1} , M^{-2} , or M^{-3} , depending on the

(26) Scatchard, G. *Ann. N.Y. Acad. Sci.* **1949**, *51*.

(27) Fanali, S. J. *Chromatogr., A* **1997**, *792*, 227–267.

(28) Colton, I. J.; Carbeck, J. D.; Rao, J.; Whitesides, G. M. *Electrophoresis* **1998**, *19*, 367–382.

overall stoichiometry. Strictly speaking the binding constants are unitless. The units are used in this work only to follow the conventions practiced in most current literature.

There are also cases where the concentration of ligand present in the BGE is much greater than that of protein in BGE ($[L]_t \gg [P]$), in which case the binding sites on the protein molecules are saturated, and the concentration of the unsaturated species ($[PL]$, $[PL_2]$, ..., $[PL_{n-1}]$) are negligible. Equation 13 can be simplified in these situations as the following:

$$I = \frac{nK_n [L]_f^n}{1 + K_n [L]_f^n} \quad (14)$$

Due to the similarities of the CE techniques, these equations can be also applied to Hummel–Dreyer (HD) and vacancy peak (VP) methods for the determination of binding parameters in either cooperative or noncooperative multiple-site protein–ligand interactions.²¹

EXPERIMENTAL SECTION

Peptide Synthesis. All peptides were made on 2-Cl₂trt resin (EMD Biosciences, San Diego, CA), using 9-fluorenylmethyloxycarbonyl (Fmoc) strategy solid-phase peptide synthesis. *O*-Benzotriazole-*N,N,N',N'*-tetramethyl-uronium-hexafluoro-phosphate (HBTU) (Advanced Chemtech, Louisville, KY) and *N*-hydroxybenzotriazole (HOBT) (Advanced Chemtech, Louisville, KY) activating agents were used, and the pH was adjusted with triethylamine (TEA) (Aldrich Milwaukee, WI). All solvents were from Fisher Scientific (Nepean, ON, Canada).

Linear peptides were cleaved in a solution of 0.1% TFA (Aldrich, Milwaukee, WI)/DCM with triisopropyl silane (TIS) (Aldrich, Milwaukee, WI) as H₂O₂ scavengers. Lyophilized linear peptides were cyclized at a concentration of 0.5 mM in dimethylformamide (DMF) using benzotriazol-1-yl-oxytripyrrolidinophosphonium hexafluorophosphate (PyBop) (Aldrich, Milwaukee, WI) and HOBT activating agent, activated in situ with TEA. Cyclization yields were typically over 95% and occurred within 30 min as indicated by an increase in retention to C18 when analyzed by reversed phase (RP) HPLC. Electrospray ionization-mass spectroscopy (ESI-MS) data showed a loss of one water molecule providing evidence of head-to-tail cyclization. ¹H NMR assignments for all amide bonds confirmed a cyclic compound. Selective deprotection of lysine side chain amines was achieved by hydrogenation with a Pd/C catalyst under normal pressure. Conjugation to the Alexa Fluor-488 preformed PFP ester (Invitrogen, Burlington, Ontario Cat. No., A-30005) was performed in mildly basic conditions and purified by RP HPLC on a C18 semi-prep column (Vydac, 214TP510) with a gradient of 0–65% aqueous acetonitrile containing 0.1% TFA. Deprotection of the final peptide was done using a solution of 95% TFA, 2.5% TRIS, and 2.5% H₂O and purified by RP HPLC using the same gradient as that for the protected and labeled peptide. The final product was eluted from a C18 semi-prep column at 21% aqueous acetonitrile for both cRADfK-488 and cRGDfK-488. All peptides were used with >95% purity, as justified by analytical HPLC and CE. Product identification was validated by ESI-MS. Peptides were lyophilized and weighed, and a standard curve for peptide quantification was established using HPLC peak areas.

Chemicals and Solutions. Purified human integrin $\alpha_v\beta_3$ (M.W. 2.37×10^5 Da) in 20 mM Tris-HCl, pH 7.5, 150 mM NaCl, 2 mM MgCl₂, and 0.2% Triton X-100 was purchased from Chemicon International (Temecula, CA, catalog no. CC1019). The initial concentration was 210 $\mu\text{g}\cdot\text{mL}^{-1}$. Integrin $\alpha_v\beta_3$ was aliquoted into portions of 10 μL and stored at -80°C . For each CE-FA experiment, the integrin was used at a concentration of 0.295 μM .

The same buffer solution was prepared and used as the background electrolyte (BGE) throughout the CE experiments. The following chemicals were used in buffer preparation: trizma base (T-8404, Sigma-Aldrich, St. Louis, MO), sodium chloride (37,886-0, Aldrich, Milwaukee, WI), magnesium chloride (Fisher Scientific, Fair Lawn, NJ), Triton X-100 (T-9284, SigmaUltra, St. Louis, MO), and hydrochloric acid (Fisher Scientific, Nepean, ON, Canada).

Purified peptides were redissolved in the aforementioned BGE at 36.03 μM and then diluted to required concentrations.

CE Conditions and Procedures. The experiments were performed on a Beckman Coulter P/ACE Glycoprotein System (Beckman Coulter Inc., Fullerton, CA) with a laser induced fluorescence (LIF) detector (488 nm excitation and 520 nm emission). An uncoated fused-silica capillary (Polymicro Technologies, Phoenix, AZ) with an inner diameter of 50 μm , an outer diameter of 360 μm , and a length of 50 cm was used. The capillary length from the injection end to the detector (effective length) was 40.2 cm.

Prior to use, the new capillary was rinsed with 1 M NaOH (30 min), methanol (30 min), purified water (30 min), and finally the separation BGE (30 min) and was conditioned with the BGE overnight. At the beginning of each run, the capillary was rinsed with 1 M NaOH (5 min), followed by methanol (5 min) and then water (5 min) and the BGE (8 min). The capillary temperature was maintained at 25 $^\circ\text{C}$. A voltage of +10 kV (anode is on the inlet side) was applied for CE runs. All experimental electropherograms were exported as ASCII files and then plotted with SigmaPlot 10.0 (Systat Software Inc., Richmond, CA).

The calibration curve of fluorescence signal vs Alexa Fluor-488 labeled peptide concentration was first constructed. The initial peptide solution (36.03 μM) was diluted to 24.02, 4.80, 2.40, 1.20, 0.48, 0.24, 0.12, and 0.08 μM . To construct the calibration curve, a relative long plug of one of the diluted peptide solutions was injected under a pressure of 0.5 psi (3447 Pa) for 90 s. Then a voltage of +10 kV was applied across the entire capillary, and the fluorescence signals were recorded. Each peptide solution was tested at least three times to minimize instrumental errors.

Proper amounts of the peptide solution and the BGE were added into one aliquot of integrin solution (10 μL) and then mixed thoroughly but gently. The mixture was placed into the sample tray of the CE instrument, and the temperature was maintained at 37 $^\circ\text{C}$ for 1 h. The pre-equilibrated mixture of integrin and peptide was injected into a neat-BGE-filled capillary under a pressure of 0.5 psi (3447 Pa) for 50 to 90 s, and then a voltage of +10 kV was applied when both inlet and outlet vials contained the BGE.

RESULTS AND DISCUSSION

CE Frontal Analysis. A good linear relationship was obtained for fluorescence signals and peptide concentrations, as proven by the R^2 value (>0.999). The calibration curve is used to determine

peptide concentrations from fluorescence signals. No signal for $\alpha_v\beta_3$ was recorded with LIF detection since the integrin is not fluorescently labeled.

A schematic illustration of the CE-FA signal and a set of real electropherograms generated from CE-FA experiments are given in Figure 1A and 1B, respectively. Figure 1A depicts the ideal signals from the free and bound peptide measured from electropherograms. Due to the amount of complex formed in the pre-equilibrated sample, the concentration of free peptide, $[L]_f$, decreases, and the height of the free peptide plateau also decreases compared to the plateau obtained for the sample containing peptide only. In Figure 1B, the higher narrow plateau (dash-dot curve) was generated from a sample containing cRGDfK-488 (2.40 μM) only. The electropherograms shown with lower and broader plateaus (solid curve and short-dash curve) in the figure were obtained from the separation of the pre-equilibrated mixture of $\alpha_v\beta_3$ integrin and cRGDfK-488. The two CE-FA curves containing broader plateaus have similar plateaus on the right side, generated by the free peptide from the mixture. With a longer plug length (90 s injection), a significant amount of complex still existed in the plug at the end of the run, giving rise to a peak on the left side. When a shorter plug length (50 s injection) was used, almost all of the complex in the mixture was dissociated during the migration, resulting in a slope on the left. The obtained electropherogram also shows that the complex migrates at nearly the same velocity as that of the free (unbound) $\alpha_v\beta_3$, but faster than the free peptide. In addition, as depicted in Figure 1B, a fairly fast dissociation rate of the $\alpha_v\beta_3$ -peptide complex is observed.

Binding Parameters. To determine the specific binding of cRGDfK-488 to human integrin $\alpha_v\beta_3$, another cyclic peptide, cRADfK-488, which is known to have no specific affinity to $\alpha_v\beta_3$, was used as a negative control. The alanine side chain of RAD in place of glycine in RGD diminishes the antagonistic ability while retaining nonspecific interactions of the peptide with the integrin.²⁹ It is important to note that it is necessary to have a ligand with a similar structure but without the specific binding affinity as a control in order to differentiate specific binding from nonspecific binding. For nonspecific binding the $[L]_b/[P]_t$ increases linearly with $[L]_f$. When the curve of $[L]_b/[P]_t$ vs $[L]_f$ of another ligand shows characteristics of a rectangular hyperbola in the linear concentration range of the nonspecific binding ligand, it is a result of specific binding. The binding isotherms of cRGDfK-488 to the integrin $\alpha_v\beta_3$ and the nonspecific binding of cRADfK-488 are shown in Figure 2. To only account for the specific binding, I_{specific} for cRGDfK-488 was calculated using the difference between the number of cRGDfK-488 bound per integrin and that of cRADfK-488, and $[L]_f$ is taken from $[L]_t - [L]_b$. This assumption is only valid if the $I_{\text{nonspecific}}$ for cRGDfK-488 is similar to $I_{\text{nonspecific}}$ for cRADfK-488.

A series of comparison studies were done as various interaction stoichiometries were assumed, and the binding isotherms constructed for integrin–RGD interaction are demonstrated in Figure 3. Equation 13 was used to fit 1:1, 1:2, and 1:3 binding isotherms of protein–ligand interaction. Binding isotherm (a) (dash-dot line) in Figure 3 is generated with an assumed 1:1 protein–ligand stoichiometry. The curve only fits the data points where the

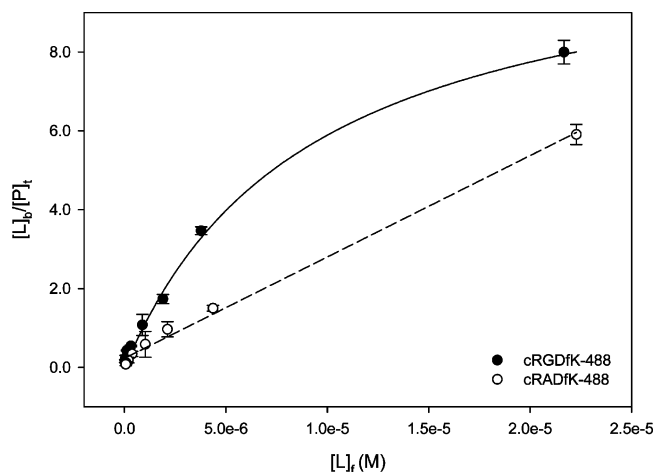


Figure 2. Binding isotherms of cRGDfK-488 and cRADfK-488 to $\alpha_v\beta_3$ integrin. Closed circles represent total binding of cRGDfK-488, and open circles represent the linear nonspecific binding of cRADfK-488 to the same amount of $\alpha_v\beta_3$.

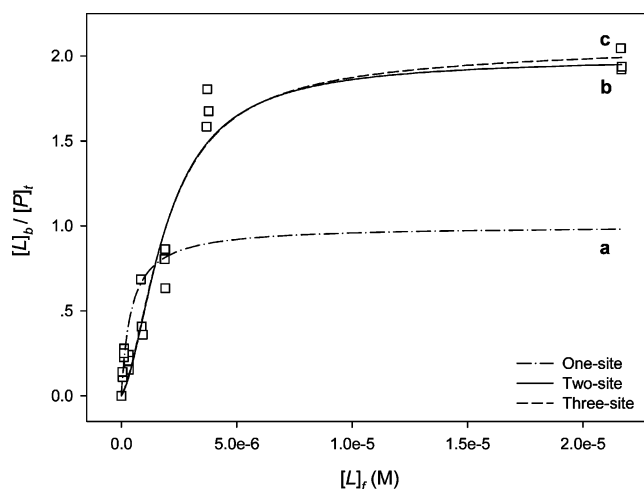


Figure 3. Specific binding isotherms of cRGDfK-488 to $\alpha_v\beta_3$ integrin. The open squares represent the specific response of cRGDfK-488. Different stoichiometries are fitted based on the experimental obtained data for (a) 1:1, (b) 1:2, and (c) 1:3 binding interactions.

concentration of ligand in the buffer is low, because 1:1 interaction is dominant in these conditions. However, values higher than 1 for I at higher ligand concentrations suggest that higher order interactions become important at higher ligand concentrations. Curve (b) (the solid line) is fitted with eq 10 when assuming two different binding sites present on each $\alpha_v\beta_3$ integrin molecule. The information provided by nonlinear regression suggests that, during CE process, two different binding sites on each $\alpha_v\beta_3$ integrin molecule can be detected with different affinities. The estimated binding constants for the two sites, K_{b1} and K_{b2} , are 2.1×10^5 and $1.3 \times 10^6 \text{ M}^{-1}$, respectively. The two sites on the $\alpha_v\beta_3$ molecules are saturated gradually as the ligand concentration in the sample mixture increases in free solution. It is obvious that the equation considering step-by-step two-site binding better describes the experimental data for the interaction of the $\alpha_v\beta_3$ integrin and cRGDfK-488. To further confirm the binding stoichiometry of the system, the data are also fitted with a 1:3 binding stoichiometry. With eq 11, the generated isotherm (c) (the short dash line) presented in Figure 3 gives a similar fitting as curve (b). The estimated binding constants for the three sites are $2.4 \times$

(29) Pfaff, M.; Tangemann, K.; Muller, B.; Gurrath, M.; Muller, G.; Kessler, H.; Timpl, R.; Engel, J. *J. Biol. Chem.* **1994**, *269*, 20233–20238.

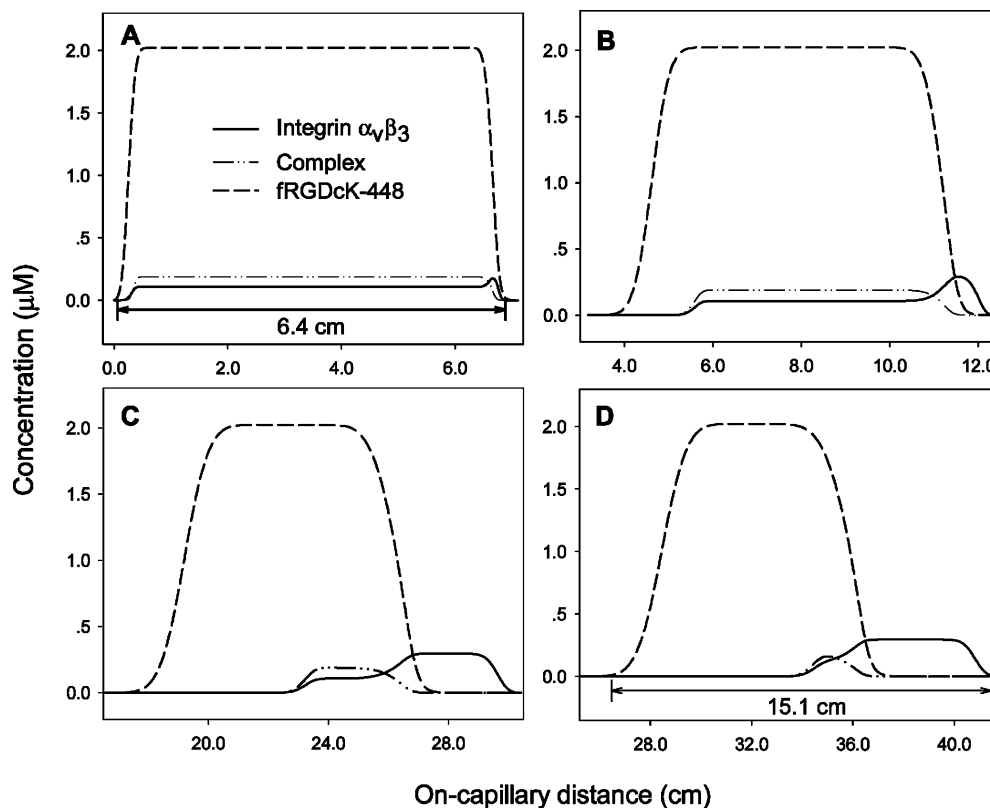


Figure 4. Simulated concentration profiles for CE-FA. Injected sample: pre-equilibrated mixture of $0.297 \mu\text{M}$ integrin $\alpha_v\beta_3$ and $2.402 \mu\text{M}$ RGD in the buffer. Injection time: 90 s. Separation voltage: 10 kV. $K_{b,\text{total}} = 2.629 \times 10^{11} \text{ M}^{-2}$. The concentration profiles of the three species are displayed in time sequence: (A) 4.0 s, (B) 100.0 s, (C) 400.0 s, (D) 755.0 s. Detailed discussions can be found in the text.

10^5 , 1.1×10^5 , and $2.3 \times 10^3 \text{ M}^{-1}$, respectively. Because the third binding constant is 2 orders of magnitude lower than the first two, it can be attributed to the slightly increased nonspecific binding at higher ligand concentrations. Therefore, it is concluded that the affinities of the two specific binding sites to the ligand are similar, reflected by the similar values of the binding constants for the first and the second steps. In theory CE-FA can be used for characterizing interactions with both strong and weak interactions and is not particularly limited by fast and slow kinetics. It is required, however, that the mobility of the complex has to be similar to either the mobility of the free protein or the free ligand to avoid significant errors in the obtained constants. In addition, because it can be difficult to differentiate the boundaries between the frontal zones of the complex and the ligands when the binding constant is below 10^3 M^{-1} , ACE may be a better method for characterizing those interactions.^{22,24}

Although it is not currently possible to explain the entire binding mechanism of this pair of reactions, the shape of the electropherograms can be explained by using our simulation program.³⁰ To understand the interaction process of the species during the electrophoresis process, a dynamic complexation capillary electrophoresis simulation program (SimDCCE) is used to study the migration of the species in a graphic format during the CE process.^{30,31}

The electrophoretic mobility of free RGD ($\mu_{\text{ep,L}}$) was determined by the following procedure: the capillary was first filled with plain buffer, then a small plug of RGD was injected for 3 s at

0.5 psi, and finally the migration time of the sample plug was measured while a voltage of 10 kV was applied across the capillary. This procedure was repeated 10 times on different days to include instrumental and other errors, and the average free mobility was determined for cRGDfK-488. The measured average electrophoretic mobility was $(2.441 \pm 0.003) \times 10^{-4} \text{ cm}^2 \text{ V}^{-1} \text{ s}^{-1}$. The mobilities of the $\alpha_v\beta_3$ integrin and integrin–RGD complex are not measurable with the LIF detector. However, they can be estimated from the mobility of bound ligands, which is the same as the complex, from the electropherograms and verified using the computer simulation program (SimDCCE).³¹ The mobilities of the integrin and complex are similar but greater than $\mu_{\text{ep,L}}$ in this case.

Four snapshots taken from a CE-FA simulation run at selected moments were exported and analyzed in Figure 4 to demonstrate the interaction and concentration changes of each species during the CE process. A relatively large volume of a pre-equilibrated mixture of $0.297 \mu\text{M}$ $\alpha_v\beta_3$ integrin and $2.40 \mu\text{M}$ RGD in the buffer was introduced into the capillary filled with neat buffer in the simulation program. As demonstrated in Figure 4A, the injected pre-equilibrated sample mixture plug is 6.4 cm, which contains $1.893 \times 10^{-7} \mu\text{M}$ integrin–cRGDfK-488 complex formed during pre-equilibrium and remaining free $\alpha_v\beta_3$ integrin and peptide. Due to the mobility order of the species ($\mu_{\text{ep,P}} \approx \mu_{\text{C}} > \mu_{\text{ep,L}}$), the integrin and complex move ahead of RGD and exit the sample plug from the front edge (Figure 4B). To maintain the equilibrium condition in the buffer solution, more cRGDfK-488 and integrin

(30) Fang, N.; Chen, D. D. Y. *Anal. Chem.* **2005**, *77*, 840–847.

(31) Fang, N.; Chen, D. D. Y. *Anal. Chem.* **2006**, *78*, 1832–1840.

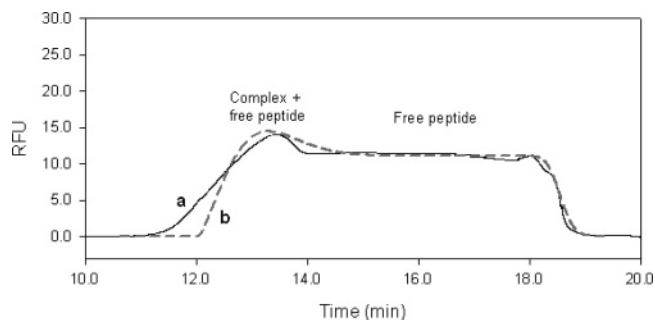


Figure 5. Comparison of the experimental result (solid line, a) with the simulation result (short dash line, b) for one of the CE-FA runs. BGE: freshly prepared buffer pH 7.5. Injected sample: 0.297 μM integrin $\alpha_v\beta_3$ and 2.402 μM RGD in the buffer. Injection time: 90 s. Separation voltage: 10 kV. $K_{b,\text{total}} = 2.629 \times 10^{11} \text{ M}^{-2}$. The injection time for the simulation is adjusted to account for the parabolic flow profile at the front of the real injection plug generated during the pressure injection.

are dissociated from the complex when the complex migrates through the cRGDfK-488 plug. As the species migrate along the capillary, they are further separated and the amounts of free peptide and integrin dissociated from the complex increase as indicated in Figure 4C. Eventually, the concentrations of each species no longer change, and a steady-state condition is established throughout the capillary. Due to the mobility difference of the species and diffusion effects, the length of the sample plug increases to 15.1 cm. The final concentration profiles are shown in Figure 4D. With SimDCCE, the final simulation result is generated as the summation of the concentration profiles of each species. With the consideration of different fluorescence intensities for each species, the simulated and experimental electropherograms for one of the CE-FA runs are compared in Figure 5. The experimental electropherogram is displayed as it is obtained, and the simulated electropherogram has been converted so that the height of the plateau matches the height of the experimental peak.

(32) Takagi, J.; Strokovich, K.; Springer, T. A.; Walz, T. *EMBO J.* **2003**, *22*, 4607–4615.

(33) Mould, A. P.; Barton, S. J.; Askari, J. A.; McEwan, P. A.; Buckley, P. A.; Craig, S. E.; Humphries, M. J. *J. Biol. Chem.* **2003**, *278*, 17028–17035.

(34) Montet, X.; Funovics, M.; Montet-Abou, K.; Weissleder, R.; Josephson, L. J. *Med. Chem.* **2006**, *49*, 6087–6093.

The experimental and simulated migration profiles and the areas of the plateau are similar.

CONCLUSION

Our CE-FA studies propose for the first time that the specific binding of cRGDfK-488 to the human integrin $\alpha_v\beta_3$ is a 1:2 interaction.

Several existing studies have demonstrated that the binding process between integrins and RGD ligands is complex. For example, studies on the association of the natural $\alpha_5\beta_1$ ligand, fibronectin, suggest that a synergy site exists to facilitate binding to the RGD site.³² It has also been shown that initial RGD–ligand binding causes a major change in the integrin’s structure in order to form a high affinity complex.³³ The existence of another binding site may also help to explain why multivalent RGD-containing imaging agents are more effective at binding to their cell target than monovalent RGD-containing agents.^{11,34}

CE provides a unique advantage for the study of membrane proteins which are inherently difficult to solubilize without disturbing the protein’s tertiary structure. It is of interest to overcome these handling problems since the most accessible targets for intravenous drug delivery reside at the surface of a cell. Perhaps more importantly, we demonstrated a new approach to processing data obtained from one of the simplest CE methods, CE-FA, to deduce important binding characteristics of biomolecules. To understand the binding of membrane proteins with complex biological behavior, nonperturbing analytical methods such as CE-FA may prove to be increasingly useful.

ACKNOWLEDGMENT

This work was supported by grants from the Natural Sciences and Engineering Research Council of Canada and the Canadian Institutes of Health Research. The authors thank Ersilia De Lorenzi of the University of Pavia for insightful discussions on CE-FA.

Received for review July 30, 2007. Accepted February 18, 2008.

AC701604A